

Study on the Effect of Combustor Scale in Annular RDEs

Moeno Miyashita¹, Akiko Matsuo¹, Eiji Shima¹,
Noboru Itouyama², Akira Kawasaki³, Ken Matsuoka², Jiro Kasahara²

¹Department of Mechanical Engineering, Keio University
Hiyoshi, Kohoku-ku, Yokohama, Kanagawa, Japan

²Department of Aerospace Engineering, Nagoya University
Furo-cho, Chikusa-ku, Nagoya, Aichi, Japan

³Department of Mechanical Engineering, Shizuoka University
Jyohoku, Naka-ku, Hamamatsu, Shizuoka, Japan

1 Introduction

A Rotating Detonation Engine (RDE) is one of the new propulsion systems currently under development, which conventionally has an annular combustor with circumferential detonation propagation. It is expected to be possible to simplify the structure by not needing converged nozzles or throats to achieve high thrust. By these backgrounds, RDE has been getting attention in recent years and several improved RDEs also have been proposed, such as cylindrical RDE [1]. However, the phenomena actually occurring inside RDE are complicated by a number of conditions, more detailed analysis is required for practical use. For example, the effect of side wall curvature on detonation propagation in RDE have not yet been clarified. The radius of cylindrical RDE combustors currently used in experiments is about 10 mm [2], the practical application of RDEs is expected to require the development of combustors on a larger scale than those currently used in experiments.

The purpose of this study is to investigate the effect of combustor curvature on detonation propagation and propulsive performance. In this paper, three dimensional numerical analyses are performed with different curvature: annular combustors, whose radii of curvature at the outer wall are 10 mm, 15 mm, and 20 mm, a cylindrical combustor, whose radius of curvature of the outer wall is 10 mm, and linear detonation channels, whose radius of curvature are infinity. In addition to these results, the effect of wall curvature was further investigated by conducting additional numerical analyses considering the effect of viscosity.

2 Numerical Setup

In this study, the three-dimensional compressible Euler equation and the conservation laws for nine chemical species (H_2 , O_2 , H , O , OH , H_2O , HO_2 , H_2O_2 , and N_2) shown below were used as the governing equations for the numerical analysis. p is the pressure, e is the total energy per unit volume, and the subscript i indicates physical quantities of i th chemical species. To enclose this system, the equation of state was used assuming thermally perfect gases condition shown below where R is the gas constant and T is the temperature.

$$\frac{\partial \hat{\mathbf{Q}}}{\partial t} + \frac{\partial \hat{\mathbf{E}}}{\partial \xi} + \frac{\partial \hat{\mathbf{F}}}{\partial \eta} + \frac{\partial \hat{\mathbf{G}}}{\partial \zeta} = \hat{\mathbf{S}}$$

$$\hat{\mathbf{Q}} = \frac{1}{J} \begin{bmatrix} \rho \\ \rho u \\ \rho v \\ \rho w \\ e \\ \rho_i \end{bmatrix}, \quad \hat{\mathbf{E}} = \frac{1}{J} \begin{bmatrix} \rho U \\ \rho u U + \xi_x p \\ \rho v U + \xi_y p \\ \rho w U + \xi_z p \\ (e + p)U \\ \rho_i U \end{bmatrix}, \quad \hat{\mathbf{F}} = \frac{1}{J} \begin{bmatrix} \rho V \\ \rho u V + \eta_x p \\ \rho v V + \eta_y p \\ \rho w V + \eta_z p \\ (e + p)V \\ \rho_i V \end{bmatrix}, \quad \hat{\mathbf{G}} = \frac{1}{J} \begin{bmatrix} \rho W \\ \rho u W + \zeta_x p \\ \rho v W + \zeta_y p \\ \rho w W + \zeta_z p \\ (e + p)W \\ \rho_i W \end{bmatrix}, \quad \hat{\mathbf{S}} = \frac{1}{J} \begin{bmatrix} 0 \\ 0 \\ 0 \\ 0 \\ 0 \\ \omega_i \end{bmatrix}$$

$$p = \sum_i \rho_i R_i T$$

The convection term was discretized by AUSMDV third ordered by MUSCL method, and three steps third ordered TVD Runge-Kutta method was used for the time integration of the fluid. The chemical reaction model proposed by Hong et al. [3] was used, which considered 20 elementary reactions of 9 chemical species, and the point-implicit method was used as the time integration method for the source term.

3 Calculation Targets

All combustors used in this study are shown in Table 1. In this research, annular combustors, linear detonation channels and a cylindrical combustor were analyzed. The height of all combustors was set in 40 mm. The constant pressure of 10 kPa was set for outer region. At the bottom of each combustor, two rows of injectors with a diameter of 1.2 mm [2] were arranged. At the injector surface, $2H_2$ - O_2 - $3.76N_2$ premixed air was injected where the total pressure and temperature were set to 1 MPa and 298 K. The pressure and temperature at the choked inflow were 0.528 MPa and 248.4 K, and the reaction induction length and C-J velocity in this unburned mixture condition were 201.9 μm and 2012 m/s.

Table 1: Summary of the combustors.

case	combustor shape	radius of outer wall [mm]	combustor width [mm]	combustor volume [10^3 mm^3]	number of injectors
A-10	annular	10	5	4.7	12×2
A-15	annular	15	5	7.9	20×2
A-20	annular	20	5	11.0	28×2
L-5.0	linear	-	5	9.4	24×2
L-6.5	linear	-	6.5	12.3	24×2
C-10	cylindrical	10	-	12.6	24×2

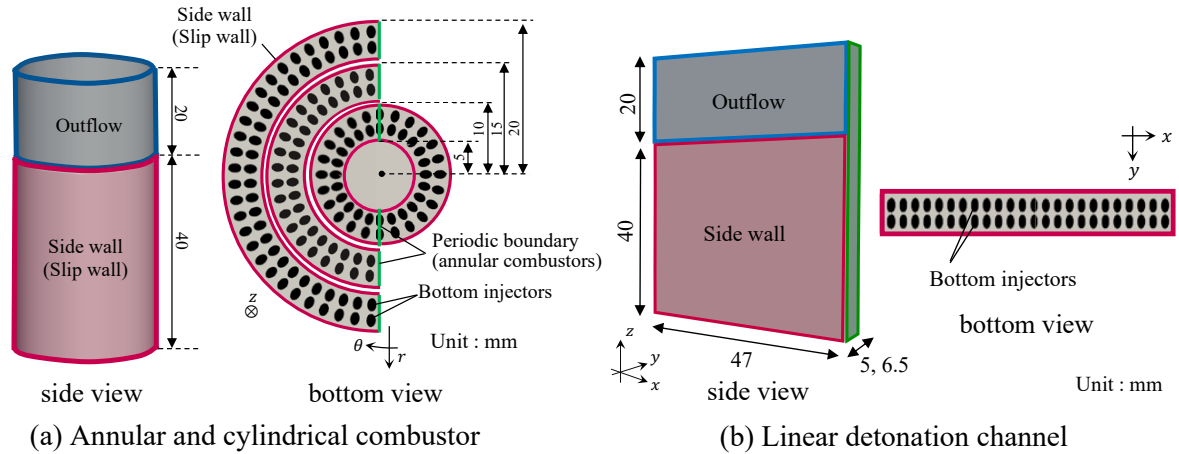


Figure 1: Calculation domain and condition of each combustor. (a) Annular and cylindrical combustor. (b) Linear detonation channel.

3.1 The annular combustors

The annular combustors used in these analyses are shown in Table 1 cases (A-10), (A-15) and (A-20), and Fig. 1. In this report, the computational domain was half the circumference of the combustor used in the actual combustor to reduce calculation cost. The radius of curvature of the outer wall was 10 mm, 15 mm, and 20 mm in three cases. The number of injectors was set to 12×2 , 20×2 , and 28×2 respectively, so that the number of injectors relative to the combustor volume would be the same in case(A-10), (A-15) and (A-20). The outer and inner wall boundary were set as slip wall. In addition, a periodic boundary was also used to simulate the continuous propagation of detonation. The number of grid points in the cases were 36.7, 61.1, and 85.6 Mpts.

3.2 The linear detonation channels

The information of linear detonation channels used in these analyses is shown in Table 1 cases (L-5.0) and (L-6.5), and Fig. 1. The linear detonation channels were the zero curvature in this report. 24 pairs of injectors were placed at the bottom. The x -directional length of the combustor was 47.1 mm, adopting the circumferential length of $r = 7.5$ mm of case (A-10). In case (L-6.5) the y -directional length of the linear detonation channel was set to 6.5 mm so that the combustor volume for the number of injectors was approximately the same as case (C-10). In contrast, the y -directional length in case (L-5.0) was set to 5.0 mm the same as case (A-10)-(A-20). The boundary condition of two combustor side walls were set as slip wall. In addition, a periodic boundary was also used the same as the annular combustors. The number of grid points in each case were 36.7 and 61.1 Mpts., respectively.

3.3 The cylindrical combustor

Case (C-10) in Table 1 and Fig. 1 shows the cylindrical combustor used in these analyses. The radius of cylindrical combustor was 10 mm in reference to the combustor in experiment by Yokoo et al.[2]. 24 pairs of injectors were placed at the bottom of the combustor. The outer wall boundary condition was set as slip wall. The number of grid points was 135.3 Mpts., respectively.

4 Results and Discussion

Figure 2 (a) shows the instantaneous pressure distribution. Figure 2 (a) from case (A-10) to case (A-20) are the pressure of annular combustors at $r = 7.5$ mm, 12.5 mm, 17.5 mm. Case (C-10) is the pressure of cylindrical combustor at $r = 10$ mm. Cases (L-5.0) and (L-6.5) are the pressure of linear detonation channels at $y = 2.5$ mm. In Fig. 2 (b), the instantaneous pressure distribution at a distance of $z = 1$ mm from the bottom (fuel impact position) are shown. In Fig.2 (c) are the time averaged pressure distribution of r - z plane for case (A-10), case(A-15), and case (A-20) and y - z plane for case (L-5.0).

In Fig. 2 (a) for case (C-10), a single wave propagated in cylindrical combustor. In contrast, multiple waves can be observed in other cases. Comparing case (C-10) and other cases in Fig. 2 (a), the wavefront, which was a well-developed detonation propagating in case (C-10), was accompanied by a higher pressure increase. Furthermore, in case (C-10), the difference in the pressure between the high-pressure region at the wavefront and the low-pressure region well behind the wavefront was significant. In contrast, the pressure distribution was more uniform throughout the flow field in other cases.

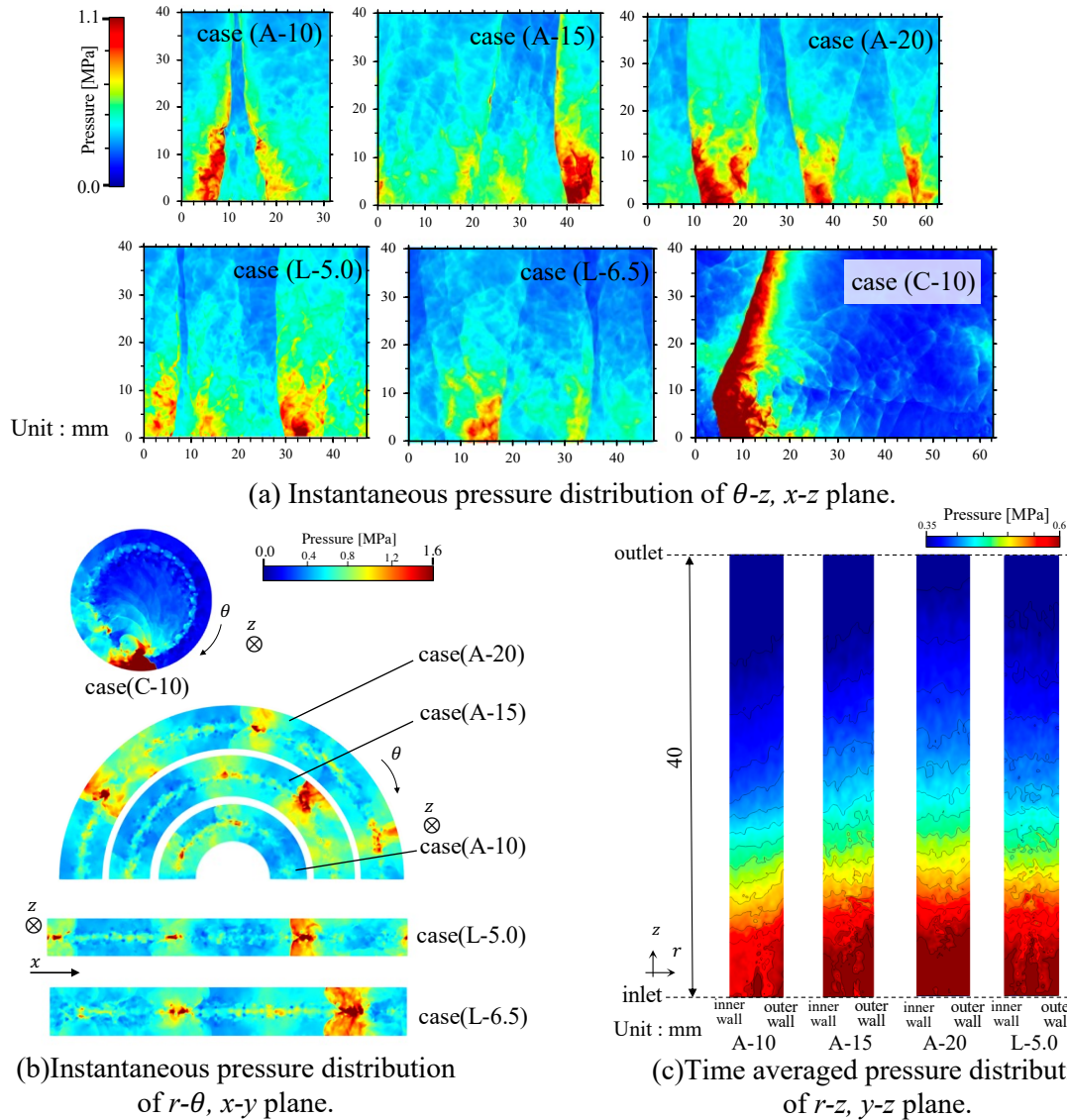


Figure 2: Pressure fields for each combustor. (a)Instantaneous fields of θ - z , x - z plane. (b)Instantaneous fields of r - θ , x - y plane. (c)Time averaged plane of r - z , y - z plane.

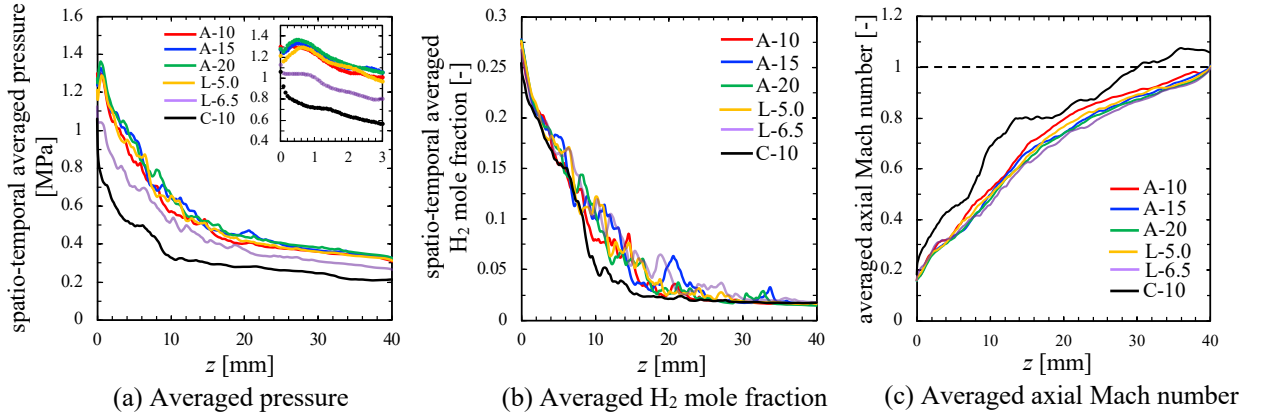


Figure 3: Spatio-temporal averaged pressure, H_2 mole fraction, and axial Mach number to the distance from the bottom to the outlet. (a) Averaged pressure, (b) Averaged H_2 mole fraction, and (c) Averaged axial Mach number.

Table 2: Mass flow rate, thrust, specific impulse, and propagation velocity for each combustor.

case	total mass flow rate \dot{m} [g/s]	mass flow rate per one injector \dot{m} [g/s]	total thrust F [N]	specific impulse I_{sp} [s]	propagation velocity D [m/s]	D/D_{CJ} [-]
A-10	47.4	1.98	78.56	168.95	1325	0.659
A-15	79.2	1.98	135.13	173.92	1288	0.640
A-20	112.8	2.01	190.28	171.96	1106	0.550
L-5.0	94.1	1.96	162.25	175.76	1043	0.518
L-6.5	101.7	2.11	172.05	172.45	959	0.477
C-10	102.5	2.13	172.74	171.79	2094	1.041

Figure 2 (b) for case (C-10) showed a slightly unsteady wavefront shape. In contrast, a distinctive symmetrical shaped wavefront can be observed in cases (L-5.0) and (L-6.5). In case (A-20), the wavefront shape was similar to cases (L-5.0) and (L-6.5), but cases (A-10) and (A-15) did not always show a symmetrical shaped wavefront with time development. In Fig. 2 (c) compared to the case (L-5.0), the pressure contours were slightly rightward in case (A-10), case (A-15), and case (A-20). The slopes of the contours are larger in the order of case (A-10), case (A-15), and case (A-20) in the range of 20 mm from the bottom. These differences in wavefront shape were thought to be caused by the difference in the curvature of combustor.

For comparison of combustor characteristics, the pressure values, H_2 mole fraction and z -axis Mach number averaged over time and space with respect to the z -axis are shown in Fig. 3. For all combustors, the averaged pressure values decreased monotonically toward the combustor outlet. From case (A-10) to case (L-5.0) with different curvature, there were no significant differences in the trends of the pressure values, and the values were similar near the combustor outlet. These trends were in good agreement with the instantaneous pressure field results in Fig. 2. In contrast, the pressure value was slightly lower in case (L-6.5), significantly lower in case (C-10) than the others. In Fig. 3. (b), The Mach number increased monotonically toward the outlet of all combustors. In case (C-10), the Mach number reached 1 at $z = 30$ mm different from the other cases. In Fig. 3 (c) for all combustors, the value of H_2 mole fraction flowed in from the bottom was decreased to the outlet by combustion. In case (C-10), the

consumption of H_2 was almost completed in the range of $z = 0-20$ mm, while in the other cases, the value of the mole fraction of H_2 showed fluctuations from the bottom to about $z = 30$ mm.

The total mass flow rate, mass flow rate per injector, thrust, and specific impulse for each combustor are shown in Table 2. Since the number of injectors was considered to be constant in relation to the combustor volume, the total mass flow rate of the unburned mixture increased as the combustor volume increased, but the mass flow rate per injector was almost constant for all combustors. The specific impulse was similar for all combustors. These results suggested that the propulsive performance was not affected even if the curvature decreases as the size of the RDE increased.

The relationship between curvature and propagation velocity during the last cycle of propagation for each combustor are also shown in Table. 2. The C-J velocity for the injector choking inflow condition was 2012 m/s. Comparing the C-J velocities to each propagation velocity, in case (C-10) of cylindrical combustor had a velocity about 4% faster, but the other combustors had velocity about 54-66% slower. In addition, the propagation velocity tended to slightly decrease as the curvature decreases.

5 Conclusion

We have numerically investigated the cylindrical and three annular RDE combustors, and two linear detonation channels using the stoichiometric hydrogen-air premixed gas whose mass flow rate per one injector were 2.02 ± 0.07 g/s. The following findings about averaged pressure, Mach number, and propulsive performance were obtained.

- A single wave propagated in a cylindrical combustor, whereas multiple waves can be observed in other annular cases.
- For all combustors, the averaged pressure values decreased monotonically toward the combustor outlet. The Mach number increased monotonically toward the outlet of all combustors. In the cylindrical case, the Mach number reached one at $z = 30$ mm, whereas it reached the outlet in other annular cases.
- The specific impulses were 172.47 ± 2.28 s⁻¹ on average in all cases. This suggested that even when the combustor size is increased, there is no decrease in propulsive performance due to the reduction in curvature.

6 Acknowledgment

This study was financially supported by JSPS KAKENHI Grants No. JP19H05464 and by the Institute of Space and Astronautical Science of the Japan Aerospace Exploration Agency. Part of the numerical results in this research were obtained using supercomputing resources at Cyberscience Center, Tohoku University.

References

- [1] Yokoo et al. (2020). Propulsion performance of cylindrical rotating detonation engine. AIAA journal. 58(12). 5107:5116.
- [2] Yokoo et al. (2022). Experimental study of internal flow structures in cylindrical rotating detonation engines. Proc. Combust. Inst. 38(3). 3759:3768.
- [3] Z. Hong, D. F. Davidson, R. K. Hanson. (2011). An improved H_2/O_2 mechanism based on recent shock tube/laser absorption measurements. Combustion and Flame. 158. 633:644.